

Analysis of Bearing Assemblies Refit in Agricultural PTO Shafts

Eleonora DESNICA*, Aleksandar AŠONJA, Milan KLJAJIN, Hrvoje GLAVAŠ, Alexander PASTUKHOV

Abstract: The paper analyzes the problems of the most commonly used cardan shafts in agricultural machinery through a theoretical review and tests on a laboratory test bench. The aim of the research presented in this paper was to define the justification of a new method for retrofitting universal joint bearing units compared to the traditional methods of retrofitting. The new approach is based on energy efficiency (saving energy, raw materials and labor) compared to the conventional methods of retrofitting. The presented investigation to justify the proposed refit was carried out after the investigation of the extent of damage to the elements of the bearing assembly, which lasted 4.02 minutes per sample, with the aim of obtaining information essential for the purpose of our work. The proposed diagnosis and refit of the cardan bearings can help to extend the service life and improve the reliability of the universal joint shafts already in service. The results of the research have shown that the method with replaceable bushings (installation of undamaged surfaces in the load transfer zone) is 6.24 to 7.54 times cheaper than the complete repair of the elements of the bearing assembly, 2.11 to 2.83 times cheaper than the refit method, in which the damaged joints are replaced with new ones, and 1.62 to 2.74 times cheaper than the purchase of new double PTO (Power Take-Off) shafts.

Keywords: damage; needle bearings; PTO shafts; repair; universal joint; wear

1 INTRODUCTION

The main purpose of the power take-off (PTO) shafts is to transmit the torque from the tractor to the working machine [1-3], where the axes of the connected shafts form an angle α [4-6], which can have a constant or a variable value. These mechanisms are widely used in agriculture, since the position of the shaft can change constantly depending on the soil conditions or the type of technological process. The power of the PTO shaft directly affects the accuracy and quality of work in agriculture [7].

The torque and power of the tractor are mainly transmitted mechanically through the PTO shafts to almost all implements and attachments (balers, seeders, mineral fertilizer spreaders, potato harvesters, etc.) [8]. The mass use of agricultural PTOs in practice, on the one hand, and the lack of repair centers for their maintenance and repair, on the other hand, show the need for significant research in this direction worldwide. In other words, the quality of machines and mechanisms is measured, among other things, by the possibility of their repair and maintenance [9]. The repair of such technical systems is justified only if the original operating conditions can be restored [10].

Reduced reliability of agricultural machinery in operation is reflected in yield losses (due to unpunctual and unsatisfactory quality of work) and increased maintenance costs (repairs, downtime, fuel, etc.). All this affects labor efficiency and leads to an increase in product price and cost per unit of labor. According to [11], tests on agricultural machinery have shown that 14% of mechanical transmission failures are due to universal joints, with about 60% of failures due to cardan joints. According to research [12], the service life of an agricultural cardan shaft is between 5 and 9 years, which is very low considering that it is used only a few days a year. This low service life is influenced by the type of maintenance and use, as well as the conditions of use (terrain, angle of rotation α , etc.) [8].

The design of complex industrial assemblies such as universal joints is very challenging due to the large number of connections that must be made between moving elements [13]. Universal joint elements are subjected to high stresses during operation. These stresses develop into

plastic deformations that can lead to permanent damage [14]. Wear is a natural, progressive process of material degradation at the contact surfaces that cannot be avoided and accompanies any tribomechanical system during power transmission under field conditions [15]. Wear processes cannot be completely eliminated, but they can be reduced to an acceptable level [16-18].

The most common conditions leading to cardan shaft damage are: unbalance [19], design defects, material fatigue [20, 21], complex working environment conditions such as dust [22], complicated maintenance [8].

In practice, the short service life of cardan shafts in agriculture is a result of, among other things: insufficient maintenance (removal of plastic protective covers by the operator, insufficient lubrication every 8 hours of operation, insufficient protection during the time when the shafts are not in operation, etc.); insufficient use (cardan shaft.) [12]; improper use (often too long or too short cardan shafts, poorly fixed shafts, too large rotation angles of the joints, application of higher torques than the shaft can withstand [23], etc.); complex atmospheric conditions [24] (working in rain, wind, dust, etc.).

2 MATHEMATICAL MODEL OF THE MOTION OF THE CARDAN SHAFT JOINT

Cardan shafts are usually made with one or two joints. In the case of shafts with only one joint, if the input and output shafts are not collinear, there will be asynchrony of rotation. In other words, when the rotational speed of the input shaft is uniform, the rotational speed of the output shaft oscillates according to the sinusoidal law. For this reason, cardan shafts with one joint are not used for power and motion transmission in agricultural machinery.

The design of the shaft with two joints connected by an intermediate shaft avoids asynchrony, reduces vibrations and dynamic loads in the area of the shaft. However, these loads due to the use of the cardan shaft contribute to damage to the elements of the cardan shaft, i.e. the universal joint.

In order to achieve asynchronism of the gearbox, it is necessary that the input, output and intermediate shafts be

in the same plane. The intermediate shaft forks should also be in the same plane. The angles between the axis of the input shaft and the intermediate shaft or between the intermediate shaft and the output shaft should be the same. Therefore, the equations of motion of the universal joint, the equations for the dependence of the angular velocities of two universal joints connected by an intermediate shaft to the input fork in the zero plane (for the spatial case) and the equations for the dependence of the angular velocities of two cardan joints connected by the intermediate shaft to the input fork in the vertical plane (for the spatial case) must be derived.

2.1 The Equation of Motion of the Cardan Joint

The kinematic analysis of the cardan joint includes the determination of the equation of motion [25]. The equation relates to the angle of rotation of the input shaft, the angle of rotation of the output shaft, and the angle between the two shafts.

During its motion, the input shaft is perpendicular to the π_1 plane and the output shaft is perpendicular to the π_2 plane (Fig. 1).

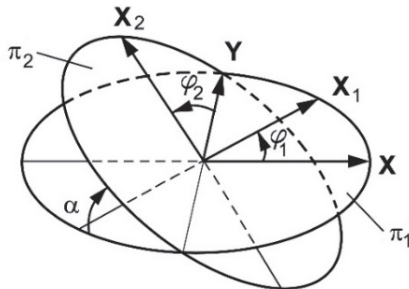


Figure 1 Relationships between vectors in the cardan joint

The vectors X and Y represent the vectors of the initial positions of the forks of the input and output shafts. During operation these vectors do not change their direction. The vectors X_1 and X_2 represent the current position vectors of the forks of the driving and the driven shaft. Let φ_1 be the rotation angle of the driving fork and φ_2 the rotation angle of the driven fork. The vector X_1 is located in the plane π_1 and is described by the expression:

$$X_1 = (\cos \varphi_1, \sin \varphi_1, 0) \tag{1}$$

The vector X_2 is located in the π_2 plane and is described by the expression:

$$X_2 = (-\cos \alpha \cdot \sin \varphi_2, \cos \varphi_2, \sin \alpha \cdot \sin \varphi_2) \tag{2}$$

where α is the angle between the driving and driven shafts.

Due to their design, the forks are perpendicular to each other. Thus, the vectors X , Y and X_1 , X_2 , are perpendicular to each other. Therefore, their scalar product is described by the equation:

$$X_1 \cdot X_2 = |X_1| \cdot |X_2| \cdot \cos 90^\circ = 0 \tag{3}$$

By inserting Eqs. (1) and (2) into Eq. (3), and by writing the resulting expression, it follows:

$$-\cos \varphi_1 \cdot \sin \varphi_2 \cdot \cos \alpha + \cos \varphi_2 \cdot \sin \varphi_1 = 0 \tag{4}$$

Dividing Eq. (4) by $\cos \varphi_1 \cdot \cos \varphi_2$, it follows:

$$-\tan \varphi_2 \cdot \cos \alpha + \tan \varphi_1 = 0 \tag{5}$$

The angle of rotation of the driven shaft is determined from Eq. (5):

$$\tan \varphi_2 = \frac{1}{\cos \alpha} \cdot \tan \varphi_1 \tag{6}$$

Eq. (6) represents the equation of motion of the cardan joint. It is evident from the equation that the angle of rotation of the driven shaft (φ_2) depends on the angle of rotation of the drive shaft (φ_1) and the angle between the drive and driven shaft (α) [26].

By deriving Eq. (6) by time, the dependence of the angular velocities of the driving and driven shafts is obtained:

$$\frac{d\varphi_2}{dt} = \frac{d\varphi_2}{d\varphi_1} = \frac{\omega_2}{\omega_1} = \frac{\cos \alpha}{1 - \sin^2 \alpha \cdot \cos^2 \varphi_1} \tag{7}$$

Before determining the expressions for the equations of the dependence of the angular velocities of the two cardan joints in the zero and vertical planes (spatial case), it is necessary to determine the equations of motion for the independent cardan joint in the zero and vertical planes. The zero and vertical planes are geometrically described according to Figs. 2a and 2b.

According to Fig. 2a, the equation of motion for an independent cardan joint in the zero plane is described by Eq. (6). The relationship between the angular velocities of the driving and driven shafts of the independent cardan joint in the zero plane is determined by Eq. (7).

According to Fig. 2b, the equation of motion for an independent cardan joint in the vertical plane is described by the expression:

$$\tan \left(\varphi_2 + \frac{\pi}{2} \right) = \frac{1}{\cos \alpha} \cdot \tan \left(\varphi_1 + \frac{\pi}{2} \right) \tag{8}$$

Since it is worth it $\tan \left(x + \frac{\pi}{2} \right) = -\cot x$, Eq. (8) takes

the form:

$$\tan \varphi_2 = \cos \alpha \cdot \tan \varphi_1 \tag{9}$$

By deriving Eq. (9) by time, the equation of the dependence of the angular velocities of the driving and driven shafts for an independent cardan joint in the vertical plane is obtained:

$$\frac{d\varphi_2}{dt} = \frac{d\varphi_2}{d\varphi_1} = \frac{\omega_2}{\omega_1} = \frac{\cos \alpha}{1 - \sin^2 \alpha \cdot \sin^2 \varphi_1} \tag{10}$$

From Eqs. (7) and (10), the angular velocities of the driven shafts are not equal to the angular velocities of the driven shafts. These two equations indicate the occurrence

of rotation asynchrony in the design of cardan shafts with one joint.

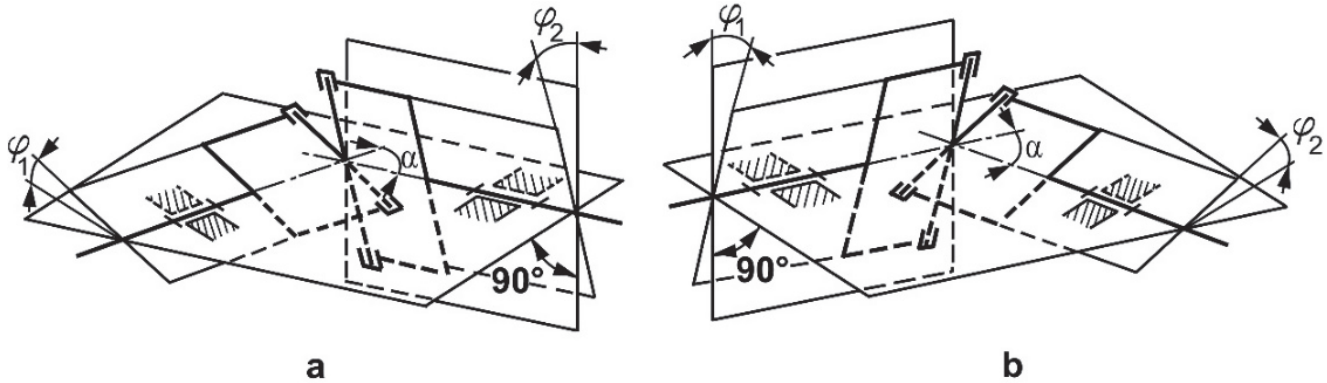


Figure 2 Zero plane (a) and vertical plane (b) according to [27]

2.2 Equations of Dependence of Angular Velocities of Two Cardan Joints Connected by an Intermediate Shaft with a Drive Fork in the Zero Plane

The spatial case of cardan shaft motion describes the motion of a shaft that uses two joints, and is applied when starting agricultural machinery. The equations of motion and dependence of angular velocities for the spatial case of the cardan shaft include the rotation angles β and γ (Fig. 3). Thus, β is the angle closed by the plane of the fork of the drive shaft and the plane of the fork of the driven shaft. The angle γ represents the angle of rotation between the forks of the intermediate shaft.

$$\sec^2(\varphi_4 + \beta) \cdot \omega_4 = \sec^2(\varphi_2 + \gamma) \cdot \omega_2 \cdot \cos \alpha, \tag{13}$$

$$\frac{\omega_4}{\omega_2} = \frac{\sec^2(\varphi_2 + \gamma)}{\sec^2(\varphi_4 + \beta)} \cdot \cos \alpha.$$

It is possible to see that the angles φ_4 and φ_1 cannot be connected to each other as in the previous cases. To achieve synchronous transmission, these two angles should be equal.

By arranging the Eq. (6), it follows:

$$\varphi_2 = \arctan\left(\frac{\tan \varphi_1}{\cos \alpha}\right) \tag{14}$$

Because it is worth it $\varphi_2 = \varphi_3$, it follows from Eq. (12).

$$\varphi_4 = \arctan(\cos \alpha \cdot \tan(\varphi_2 + \gamma)) \tag{15}$$

According to the derived expressions, it is possible to conclude that for the value of the angle $\alpha = 0^\circ$, and for $\gamma = \beta$, it follows that the angles φ_4 and φ_1 are equal ($\varphi_4 = \varphi_1$). In this case, synchronous transmission was achieved with a cardan shaft with two joints in the zero plane. For the case when the angles $\gamma = \beta$ and the angle $\alpha \neq 0^\circ$, it is not possible to achieve synchronous transmission.

2.3 Equations of Dependence of Angular Velocities of Two Cardan Joints Connected by an Intermediate Shaft with a Drive Fork in the Vertical Plane

According to Fig. 4, the equation of motion for the first cardan joint in the zero plane is described with Eq. (9).

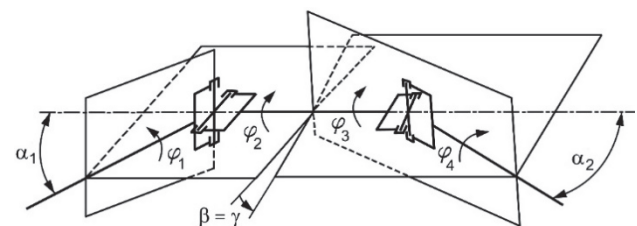


Figure 4 Drive shaft fork in the vertical plane for the spatial case

Figure 3 Drive shaft fork in the zero plane for the spatial case

According to Fig. 3, the equation of motion for the first cardan joint in the rear plane is described by Eq. (6). The second cardan joint is located in a vertical plane, so the angle of rotation of the drive fork of the intermediate shaft (φ_3) is increased by the angle γ . The angle of rotation of the driven shaft (φ_4), according to Fig. 3, is increased by the angle β . Therefore, it can be written:

$$\tan(\varphi_4 + \beta) = \cos \alpha \cdot \tan(\varphi_3 + \gamma) \tag{11}$$

The intermediate shaft represents one solid body, and is valid $\varphi_2 = \varphi_3$. Therefore, Eq. (11) has the following written form:

$$\tan(\varphi_4 + \beta) = \cos \alpha \cdot \tan(\varphi_2 + \gamma) \tag{12}$$

After derivation of Eq. (12) follows:

The second cardan joint is located in a vertical plane, so the angle of rotation of the drive fork of the intermediate shaft (φ_3) is increased by the angle γ . The angle of rotation of the driven shaft (φ_4), according to Fig. 4, is increased by the angle β . Therefore, it can be written:

$$\tan(\varphi_4 + \beta) = \frac{1}{\cos\alpha} \cdot \tan(\varphi_3 + \gamma) \quad (16)$$

It can be written as it is worth $\varphi_2 = \varphi_3$. Therefore, Eq. (16) has the following notational form:

$$\tan(\varphi_4 + \beta) = \frac{1}{\cos\alpha} \cdot \tan(\varphi_2 + \gamma) \quad (17)$$

After derivation of Eq. (17) it follows:

$$\sec^2(\varphi_4 + \beta) \cdot \omega_4 = \sec^2(\varphi_2 + \gamma) \cdot \omega_2 \cdot \frac{1}{\cos\alpha},$$

$$\frac{\omega_4}{\omega_2} = \frac{\sec^2(\varphi_2 + \gamma)}{\sec^2(\varphi_4 + \beta)} \cdot \frac{1}{\cos\alpha}. \quad (18)$$

In addition, as in the previous case, it is not possible to connect the angles φ_4 and φ_1 . To achieve synchronous transmission, these two angles should be equal [28].

By arranging the Eq. (9), it follows:

$$\varphi_2 = \arctan(\tan\varphi_1 \cdot \cos\alpha) \quad (19)$$

Since $\varphi_2 = \varphi_3$ holds, it follows from Eq. (17):

$$\varphi_4 = \arctan(\cos\alpha \cdot \tan(\varphi_2 + \gamma)) \quad (20)$$

According to the obtained expressions, for the angle $\alpha = 0^\circ$, and for $\gamma = \beta$, it follows that the angles φ_4 and φ_1 are equal. Since the angle $\alpha = 0^\circ$, the driving and driven shafts are collinear. By fulfilling the conditions of collinearity, synchronous transmission was achieved with a cardan shaft with two joints in the vertical plane. For the case when the angles $\gamma = \beta$ and the angle $\alpha \neq 0^\circ$, asynchronous transmission is achieved.

3 MATERIAL AND METHODS

The research in this paper is divided into two parts. In the first part of the research, which was conducted in the field and in the laboratory, the double PTO and drive shafts were examined to determine the degree of damage on the surface of the bearings. The second part of the research examined the economic justification for overhauling universal joints by introducing undamaged surfaces into the load transfer zone and compared it to traditional refit methods. The objective of the research described in this paper was to define the justification of a new approach to the overhaul of universal joints compared to traditional overhaul methods.

3.1 Investigations of Damages of Universal Joint Bearing Assemblies

A model of double PTO shafts was chosen to study damage to universal joint bearings in agricultural PTO shafts. Size 1 of double PTO shafts was studied, and there were five shaft patterns that were subjected to laboratory and field tests. Fig. 5 shows the 3D model of the universal joint studied.

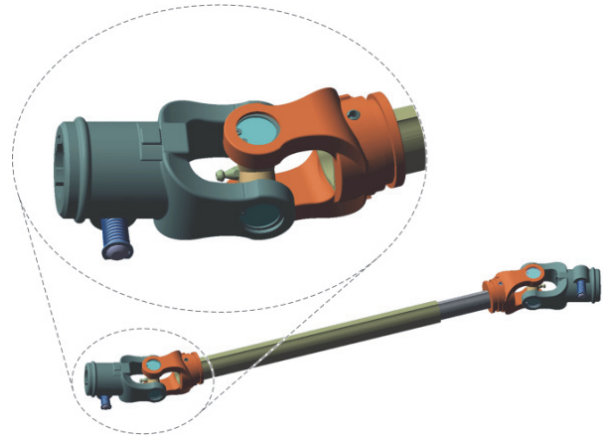


Figure 5 The mechanism studied in the paper - 3D model of a double PTO shaft

The type of connection on the forks of the test cardan shafts is a hexagonal groove made in accordance with the ASAE S203 standard. Fig. 6 shows the appearance and dimensions of a complete spherical plain bearing assembly (cross shaft, pin and cup) on the tested shaft, while Fig. 7 shows the cross section of the telescopic shaft with dimensions.

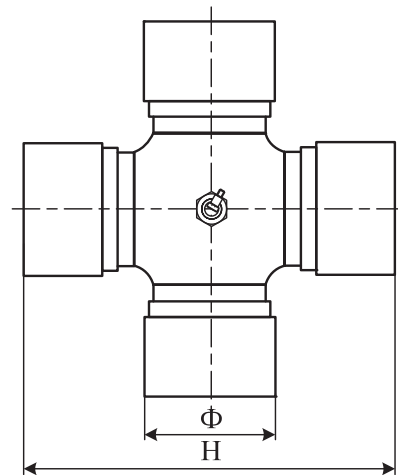


Figure 6 Appearance and dimensions of the complete bearing assembly after mounting the pins and cups on the cross shaft

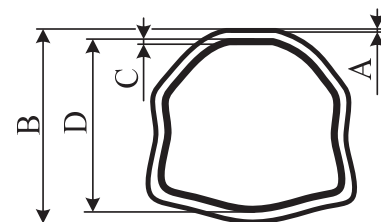


Figure 7 Dimensions of the cross-section of the examined telescopic cardan shaft

Tab. 1 shows the tested sizes of universal joint shaft.

Table 1 Examined sizes of universal joint shaft

Universal joint shaft sizes	1	2	3	4	5	6	8
\varnothing / mm	22.0	23.8	27.0	27.0	30.2	30.2	35.0
H / mm	54.0	61.3	74.6	74.6	79.4	91.4	106
A / mm	2.6	3.2	3.4	3.4	3.0	4.0	4.0
B / mm	32.5	36.0	43.5	43.5	51.5	54.0	63.0
C / mm	4.0	4.0	3.2	4.0	3.8	4.2	4.0
D / mm	26.5	29.0	36.0	36.0	45.0	45.0	54.0

Tab. 2 shows the values of the operating parameters of the tested PTO shafts, while Tab. 3 shows the values of the operating parameters of the test.

Laboratory methods were used to investigate the damage in bearing units of cardan shafts. The laboratory tests included methods for dynamic temperature investigation in bearing assemblies.

Table 2 Values of operating parameters of the tested PTO shafts

PTO operating parameters	Value
Size	1
Power P / kW	12
Moment M / N·m	210
Maximum dynamic torque M_d / N·m	320

Table 3 Values of operating parameters during laboratory testing

Test operating parameters	Value
Joint rotation angles $\alpha_{12} = \alpha_{21} / ^\circ$	20
Number of revolutions of the shaft / rpm	540
Output load / kW	4

The conclusion that the bearing assemblies failed was drawn after their examination on the laboratory test bench. The diagnosis of each sample performed on the laboratory bench lasted 4.02 minutes per sample and included the testing of temperature in bearing assemblies. The diagnostic values examined were not subject to this study, although their extreme values were used only as indicators of bearing assembly or universal joint failure. The conditions under which the reliability tests of the double PTO were carried out are as follows:

- a "Z" arrangement was used,
- the rotation was only in one direction.

The reliability tests of the cardan bearings were performed on a laboratory test stand, model: ANA Fig. 8 - a schematic diagram of the laboratory stand with marked elements and Fig. 9 - the laboratory stand [29].

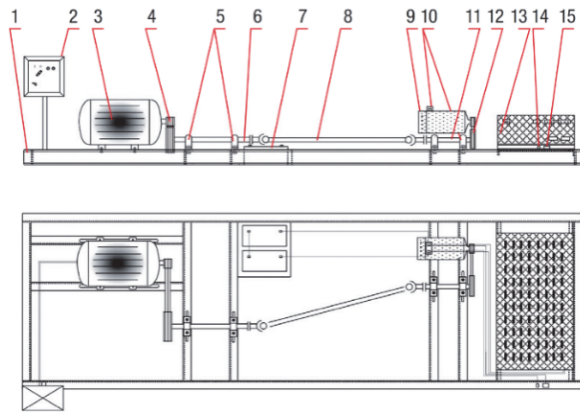


Figure 8 Schematic view of the laboratory stand with marked working elements

- 1 - steel construction
- 2 - main electrical control box
- 3 - electric motor
- 4 - gears on the drive belt area
- 5 - bearing units on the first additional shaft
- 6 - the first auxiliary shaft
- 7 - batteries
- 8 - the laboratory cardan shaft
- 9 - direct current (DC) generator
- 10 - reservoir units on the second auxiliary shaft
- 11 - second auxiliary shaft
- 12 - belt conveyors at brake part
- 13 - regulation system load
- 14 - manual control of the generator excitation DC
- 15 - control lamp excitation DC generator



Figure 9 The laboratory stand

The dynamic examination methods included methods for examining the temperature in the bearing units. The criterion for assessing the condition of bearing units by temperature was: $< 62 \text{ }^\circ\text{C}$ - satisfactory condition, $62\div 73 \text{ }^\circ\text{C}$ - unsatisfactory condition, $> 73 \text{ }^\circ\text{C}$ undesirable condition [29]. The extreme criterion of bearing unit failure was the temperature rise above $73 \text{ }^\circ\text{C}$. The paper protractors were used to measure the damage angle in universal joint bearing assemblies.

3.2 Analysis of Methods for the Justification of the Refit

The analysis of the rationale included three possible ways of renewing the bearing assemblies, as shown in Fig. 10:

- The complete repair of the elements of the bearing assembly.
- Replacement of damaged joints with new ones.

- Installation of undamaged surfaces in the load transfer zone with replacement of needle bearings, according to the patent [30]. The results of the investigation will show the degree of damage to the bearing assemblies and the possibility of carrying out this type of overhaul.

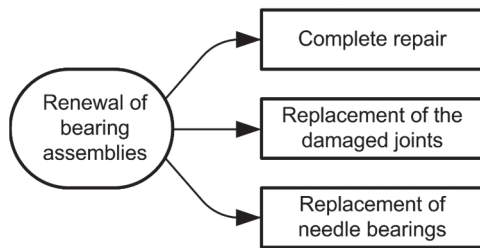


Figure 10 Methods for the justification of the refit

The complete repair of the elements of universal joints included (all costs are expressed in euros €): the costs of joint repair - C_{rz} , the costs of new needle bearings - C_{nl} and the costs of joint disassembly and reassembly - C_{dm} . The main technological procedure in the universal joint refit is the welding procedure [31]. The costs of universal joint repair - C_{rz} comprise the costs of hard facing of damaged surfaces of the cross shaft and cups by the TIG welding process, their grinding and finally, reassembling their original position. The costs of the complete repair may be expressed with Eq. (21):

$$C_r = C_{rz} + C_{nl} + C_{dm} \quad (21)$$

The replacement of the damaged joints with the new ones includes: costs of new joints - C_{nz} , joint disassembly and reassembly - C_{dm} , i.e. replacement of the damaged joints with the new ones. The costs of replacement of the damaged joints with the new ones - C_z , may be expressed with Eq. (22):

$$C_z = C_{nz} + C_{dm} \quad (22)$$

Fitting the undamaged surfaces in the load transfer zone along with replacement of needle bearings comprise: the costs of new needle bearings - C_{nl} , the costs of joint disassembly and reassembly - C_{dm} and the costs of fitting the new undamaged surfaces of the crosshead sleeves and cups in the load transfer zone - C_{up} . The costs of setting the undamaged surfaces in the load transfer zone along with replacement of needle bearings - C_{np} may be expressed with Eq. (23):

$$C_{np} = C_{nl} + C_{dm} + C_{up} \quad (23)$$

The analyzed refits and replacements of universal joints described in Eqs. (21) and (22) were conducted in the machine shops of the company named Termomontaza Novi Sad. The gross hourly price for overhaul work was 13.24 € per hour. The analyzed refit methods expressed with Eq. (3), i.e. the refits based on fitting the undamaged surfaces in the load transfer zone were conducted using the solutions offered in patented universal joints. The patents of *Professor Sigaev et al.* which have cross shaft sleeves

with pressed-in bushes of great hardness shaped as convex regular polygon [30]. The feature of the presented patent solution is the easy replacement of damaged sleeves surfaces - by rotating the sleeves i.e. placing undamaged surfaces in the load transfer zone.

The relationship between the justification of the mentioned bearing assembly refit methods and the justification of the installation of the new universal joint shafts is given in the simple regression model in Eq. (24):

$$y = \gamma + \beta(X) + \varepsilon \quad (24)$$

where: y - is costs of bearing assembly refit depending on the selected refit method (included costs from Eqs. (21) to (23)); X - is the value of a new universal joint; ε - residual; γ and β - are the model parameters (β is a parameter that tracks the relationship between the value of repair costs and the price of a cardan shaft, while the γ parameter includes initial costs unrelated to the change in the price of a new cardan shaft).

4 RESULTS AND DISCUSSION

4.1 Analysis of Damages in Universal Joint Bearing Assemblies

All bearing assembly elements tested in the field under operation conditions underwent visible damages. The most striking and evident damages were reported on the crosshead sleeve surface which were the result of the fatigue wear. Somewhat smaller but identical damages occurred on the surfaces of the bearing cups (20CrMn5), while on the needle bearings (100Cr6) there were most damaged surfaces recorded. Some examples of damages in bearing assembly elements in field operation are shown in Fig. 11. Fig. 11a shows damage of the crosshead and Fig. 11b cup damages; Fig. 11c shows the damaged needle bearings of one bearing assembly. The damages in the form of thinned surface appeared on the upper part of the sleeve at an angle of 120°, Figs. 12a and 12b, the same maximum angle of 120° appeared on the cups, Fig. 12c. The undamaged surfaces of the sleeves and cups cover an angle of 240°. One part of these surfaces at an angle of 120° would overtake the load only when the universal joint shaft rotates in the opposite direction, which means that when it rotates in the same direction, they do not wear. The weakest elements of universal joint bearing assemblies are in fact the needle bearings with the highest percentage of wear, Fig. 11c. Almost every bearing assembly had broken bearings. Such a high degree of damage of the needle bearings in universal joints together with their shape and price indicate the fact that it is necessary to install new needle bearings during every overhaul of these systems. The results of damage to the bearing assemblies were identical to the results stated in the research [32].

The damaged surfaces in the bearing assemblies (cross shaft sleeves and cups) which undergo wear, occurred at an angle of 120°, Fig. 13. The rest of the surfaces of the bearing assemblies remained almost intact. The previously described analysis leads to the conclusion that if the worn surfaces are replaced with the intact ones, the life span of universal joint shafts may be considerably extended, i.e. the refit, which includes fitting the undamaged surfaces in the load transfer zone, may be conducted two more times.

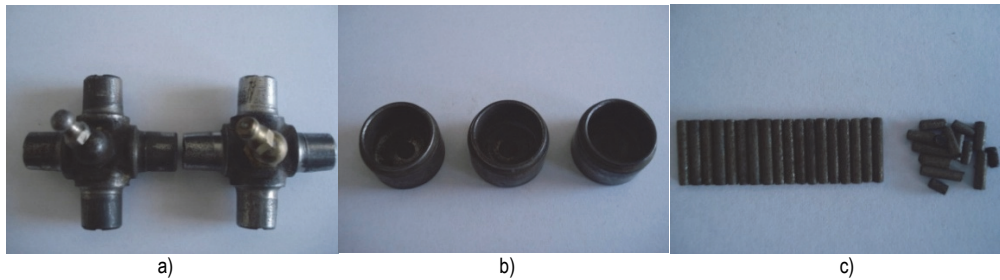


Figure 11 The damaged surfaces of rolling elements in universal joint bearing assembly samples in operating conditions: a) cross shaft; b) cups; c) bearings

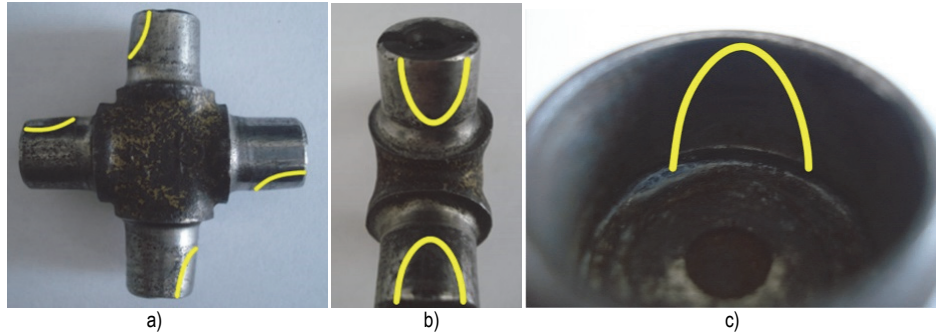


Figure 12 Zones of intensive wear of the bearing assembly elements a) on cross shaft; b) on cross shaft (side view); c) on cups

These detected damaged bearing assembly elements, primarily the crosshead and cups, evidenced a very small damage of the surfaces where the overhaul including fitting undamaged surfaces in the load transfer zone may be suggested as a method applied to increase the level of total reliability.

Two basic types of wear of universal joint bearing assemblies occurring in field operation conditions are fatigue wear (Fig. 14a) and brinelling (Fig. 14b). Fig. 14 shows the damaged working surfaces of the crosshead sleeves.

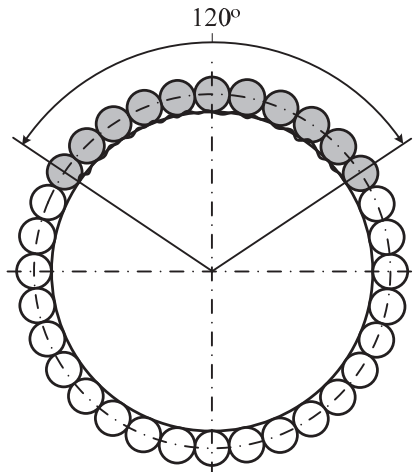


Figure 13 The angle of the damaged surface on the crossshaft sleeves

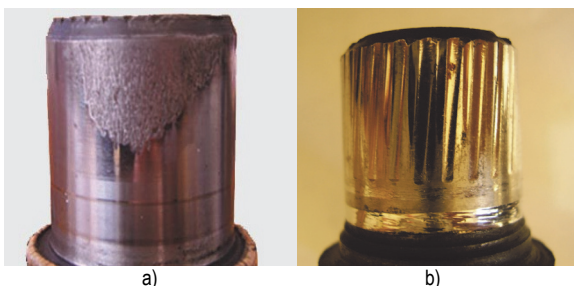


Figure 14 Damaged crosshead sleeves: a) fatigue wear; b) plastic deformations - brinelling

The damage surfaces of the cross shafts (shown in Fig. 12a and 12b) fit into the research of the calculated temperature fields on the cardan joint that were shown in the research [33], Fig. 15. In this research, the cardan joint was modelled using the finite element method in the KOMPAS-3D V18 CAD software package, and the analysis of the temperature fields was calculated using the APM FEM module. The resulting map of the calculated temperature fields is shown in Fig. 15a, while Fig. 15b shows the map of temperature fields for the cardan joint as a whole, taking into account the heat release of the four bearing assemblies.

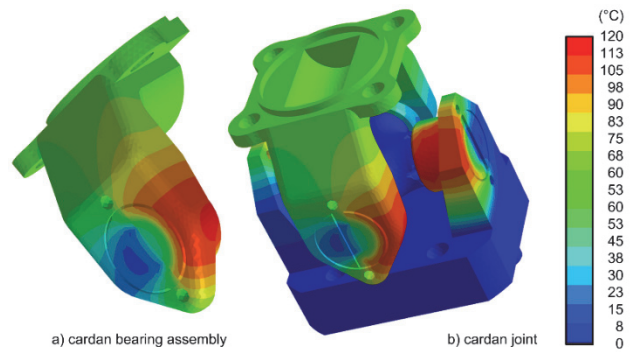


Figure 15 Visualization of stress on the cardan joint

4.2 Statistical Data Analysis of the Justification of Universal Joint Refit

Based on the empirical data about the relationship between the universal joint refit price (using the three methods described in this paper) and the price of the new universal joint shafts, Eqs. (25) to (27) for the first bearing assemblies refit, and Eqs. (28) to (30) for the second refit of the bearing assemblies of the joints on the shaft were obtained.

- The said values for the first refit of the joints are:
- for the complete repair of the universal joint elements:

$$y_{cr1} = 169.50 + 1.92(X) + \varepsilon \tag{25}$$

- for the replacement of the damaged joints with the new ones:

$$y_{mo1} = 20.31 + 0.94(X) + \varepsilon \tag{26}$$

- fitting the undamaged surfaces in the load transfer zone with replacement of the needle bearings:

$$y_{mb1} = 26.61 + 0.24(X) + \varepsilon \tag{27}$$

The said values for the second refit of the joints are:

- for the complete repair of the universal joint elements:

$$y_{cr2} = 399.00 + 1.92(X) + \varepsilon \tag{28}$$

- for the replacement of the damaged joints with the new ones:

$$y_{mo2} = 40.61 + 0.94(X) + \varepsilon \tag{29}$$

- fitting the undamaged surfaces in the load transfer zone with replacement of the needle bearings:

$$y_{mb2} = 53.22 + 0.24(X) + \varepsilon \tag{30}$$

The results of the parameters estimation, using the Gretl software package (license version 9.0 Open source), are shown in Tab. 4.

Table 4 The estimation of the parameters of the Eqs. (25) to (30)

Values	Parameters	Standard Error	P-value	R ² / %
y _{cr1}	169.505	29.714	0.231	94.21
	1.919	0.212	0.274	
y _{mo1}	20.307	6.801	0.306	98.63
	0.936	0.048	0.061	
y _{mb1}	26.615	2.368	0.073	97.58
	0.245	0.017	0.082	
y _{cr2}	399.009	59.427	0.231	94.25
	1.919	0.212	0.274	
y _{mo2}	40.614	13.602	0.306	98.69
	0.936	0.048	0.061	
y _{mb2}	53.229	4.736	0.073	97.72
	0.245	0.017	0.082	

All the obtained parameters are statistically significant for the level of confidence of 95%. The coefficients of determination (R Square) for the first refit are 94.21%, 98.63% and 97.58%, while for the second refit they are 94.25%, 98.69% and 97.72%. These percentages show the validity of the models used to describe the relationship between the values of universal joint shafts as the independent variable, and the said costs of refit methods as the dependent variable in regression models expressed with Eqs. (25) to (27) and Eqs. (28) to (30). The obtained expressions clearly show the justification of the proposed refit method, Eqs. (27) to (30) (fitting the undamaged surfaces in the load transfer zone along with replacement of the bearings), in comparison with the conventional universal joint refit method. In other words, the obtained expressions may be used in decision-making process when

a method for a universal joint shaft refit should be selected depending on its value.

4.3 Analysis of Economic Justification of Replacing the Universal Joint

The analysis of justification of universal joint bearing assembly refit by fitting the undamaged surfaces in the load transfer zone and comparison with the conventional refit is shown in Fig. 16 and 17. Fig. 16 shows the analysis of justification for the first refit (both joints) of doubly PTO drive shafts, type 1, 2, 3, 4, 5, 6 and 8 at their first failure. Fig. 17 shows the analysis of justification for the second refit (both joints) of doubly PTO drive shafts, type 1, 2, 3, 4, 5, 6 and 8 at their second failure. Figs. 16 and 17, show the prices of universal joints (Fig. 16 - 1NU - the price of a new universal joint and Fig. 17 - 2NU - the price of two new universal joints).

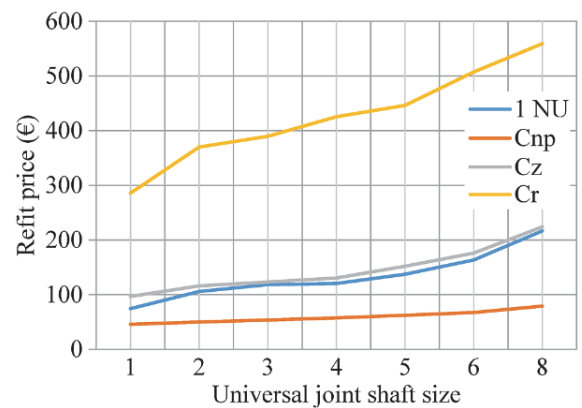


Figure 16 Justification of the first refit of universal joints (the first fitting of the undamaged surfaces in the load transfer zone)

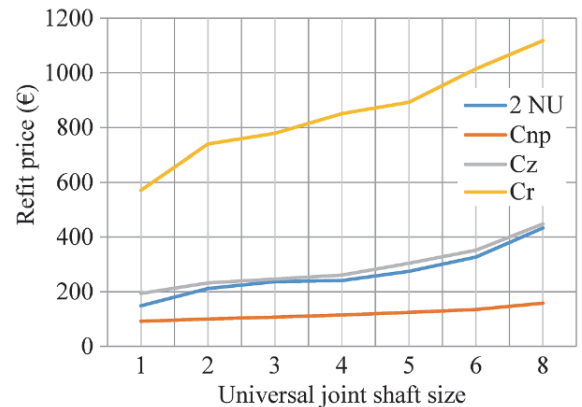


Figure 17 Justification of the second refit of universal joints (the second fitting of the undamaged surfaces in the load transfer zone)

Analyzing the repair methods described in Eqs. (21) and (22) (Figs. 16 and 17), it can be concluded that the method of complete repair of bearing assembly elements is not economically justified, that is, it is from 2.50 to 3.26 times more expensive than the method for replacement of damaged joints with new ones.

Analyzing the repair methods described in Eqs. (21) and (23) (Figs. 16 and 17), it can be concluded that the method of complete repair of bearing assembly elements is not economically justified, that is, it is from 6.24 to 7.54 times more expensive than the method for introduction of undamaged surfaces in the load transfer zone.

Furthermore, analysing the refit methods described in Eqs. (22) and (23) in Figs. 16 and 17 it can also be concluded that replacement of damaged joints with the new ones is economically justified as well. Depending on the size of the universal joint shaft, the refit which includes fitting the undamaged surfaces in the load transfer zone is between 2.11 and 2.83 times cheaper than replacement of damaged joints with the new ones, Figs. 16 and 17.

The comparison between the costs of the refit which includes fitting the undamaged surfaces in the load transfer zone, Eq. (23), and the price of new double PTO shafts, 1NU and 2NU, Fig.16 and 17, also leads to the conclusion that the proposed refit may be 1.62 to 2.74 times cheaper (depending on the size of the universal joint shaft) than the purchase of new double PTO shafts.

In addition, if the two most economically justified methods are analyzed (method which includes fitting the undamaged surfaces in the load transfer zone and the one which includes replacement of damaged joints with the new ones), it can be concluded that, depending on the size of the PTO shaft, considerable savings may be made. Thus, for the first refit, i.e. the first fitting of the undamaged surfaces in the load transfer zone, the savings ranging between 51 and 145 € may be made if compared with the refit which includes replacement of damaged joints with the new ones. The second refit, i.e. the second fitting of the undamaged surfaces in the load transfer zone, the savings ranging between 102 and 290 € may be made if compared with the refit which includes replacement of damaged joints with the new ones. If 100 doubly PTO drive shafts are refitted, the refit centres may save between 5.100 and 14.500 €, depending on the size of the universal joint shafts. Similarly, if compared with the conventional replacement of damaged joints with the new ones, the second refit, i.e. the second fitting of the undamaged surfaces in the load transfer zone may save between 10.200 and 29.000 €, depending on the size i.e. on the type of the universal joint.

5 CONCLUSION

The main results of the research described are as follows: The described repair methods have shown that the size of cardan shafts is directly proportional to the justification of the repair; further implementation of the best described overhaul model would contribute to savings in raw materials and energy; the possibility of using the research results for other mechanical elements and mechanisms subject to wear.

In order to increase the reliability of agricultural cardan shafts in field use, further research should be directed towards the development of new and the improvement of current technical solutions for universal joints. In this regard, all scientific, research and development activities should focus on the following: improvement of current technical solutions of bearing assemblies that would lead to significantly better maintenance and retrofitting, development of technical solutions of universal joints that are suitable for maintenance and retrofitting without disassembling the elements of the bearing assembly, development of sensor units - based on the Internet of Things (IoT) in cardan joints that will detect incipient damage in universal joint bearing assemblies, and improvement of current technical solutions of universal joints whose service life will be extended by

using high-quality construction material for the development of rolling elements in bearing assemblies.

The proposed diagnosis and refit of universal joint bearing assemblies can extend the service life and increase the reliability of cardan shafts in use. In addition to significant cost efficiency, other savings can be achieved, such as labour for maintenance and retooling, reducing raw material and energy consumption for the development of a universal joint, and improving operator safety.

Acknowledgments

The research is conducted through the project "Creating laboratory conditions for research, development, and education in the field of the use of solar resources in the Internet of Things", at the Technical Faculty "Mihajlo Pupin" Zrenjanin, financed by the Provincial Secretariat for Higher Education and Scientific Research, Republic of Serbia, Autonomous Province of Vojvodina, Project number 142-451-3118/2022-01.

6 REFERENCES

- [1] Mandal, S. K., Shekh, M. I., Kumar S., Chakraborty, C., & Kumar, N. (2022). Failure analysis of PTO shaft of an agricultural tractor. *Materials Today: Proceedings*. <https://doi.org/10.1016/j.matpr.2022.06.574>
- [2] Bellochio, S. D. C., Alonço, A. S., Possebon, G., Gubiani, P., & Pagliarin, L. (2019). Presence and dimensional assessment of power take-off (PTO) protection of new Brazilian agricultural tractors. *Agricultural Engineering International: CIGR Journal*, 21(3), 130-137.
- [3] Kukushkin, E. V. (2021). Equations of motion of the universal joint. *Bulletin PNRPU - Mechanical engineering, materials science*, 23(2), 79-86.
- [4] Tchomeni, B. X. & Alugongo, A. (2020). Theoretical and experimental analysis of an unbalanced and cracked cardan shaft in the vicinity of the critical speed. *Mathematical Models in Engineering*, 6(1), 34-49. <https://doi.org/10.21595/mme.2019.21240>
- [5] An, K. & Wang, W. (2017). Transmission performance and fault analysis of a vehicle universal joint. *Advances in Mechanical Engineering*, 9(5), 1-10. <https://doi.org/10.1177/1687814017707478>
- [6] Golafshan, R., Dascaluc, K., Jacobs, G., Roth, D., Berroth, J., & Neumann, S. (2021). Damage Diagnosis of Cardan Shafts in Mobile Mining Machines using Vibration Analysis. *IOP Conf. Series: Materials Science and Engineering*, 1097, 012019. <https://doi.org/10.1088/1757-899X/1097/1/012019>
- [7] Wang, Y., Wang, L., Zong, J., Lv, D., & Wang, S. (2021). Research on Loading Method of Tractor PTO Based on Dynamic Load Spectrum. *Agriculture*, 11(10), 982. <https://doi.org/10.3390/agriculture11100982>
- [8] Asonja, A. & Desnica, E. (2015). Reliability of agriculture universal joint shafts based on temperature measuring in universal joint bearing assemblies. *Spanish Journal of Agricultural Research*, 13(1), e02-001. <https://doi.org/10.5424/sjar/2015131-6371>
- [9] Milojević, S., Savić, S., Marić, D., Stopka, O., Krstić, B., & Stojanović, B. (2022). Correlation between Emission and Combustion Characteristics with the Compression Ratio and Fuel Injection Timing in Tribologically Optimized Diesel Engine. *Tehnički vjesnik*, 29(4), 1210-1219. <https://doi.org/10.17559/TV-20211220232130>
- [10] Dihovični, Dj., Asonja, A., Radivojević, N., Cvijanovic, D., & Škrbić, S. (2020). Stability issues and program support for time delay systems in state over finite time interval. *Physica*

- A: Statistical Mechanics and its Applications*, 538, 122815. <https://doi.org/10.1016/j.physa.2019.122815>
- [11] Tavlybaev, F. N. (1991). Renewal of machine parts and equipment. *The scientific and technical information proceedings 1st ed.* Informagroteh, Moscow, Russia.
- [12] Pastukhov, A. G. & Timashov, E. P. (2009). *Increasing durability of cardan joints of vehicles and machines in operation.* Stary Oskol (Russia): National University of Science and Technology, Moscow Institute of Steel and Alloy (MISI).
- [13] Ciaccioli, C. & Morabito, A. V. (2021). An investigation on skeleton-based top-down modelling approaches of complex industrial product. *Journal of Graphic Engineering and Design*, 12(1), 11-21. <https://doi.org/10.24867/JGED-2021-1-011>
- [14] Dimitris, S., Paraforos, D. S., Griepentrog, H. W., Vougioukas, S. G., & Kortenbruck, D. (2014). Fatigue life assessment of a four-rotor swather based on rainfall cycle counting. *Biosystems Engineering*, 127, 1-10. <https://doi.org/10.1016/j.biosystemseng.2014.08.006>
- [15] Patil, A. A., Desai, S. S., Patil, L. N., & Patil, S. A. (2022). Adopting artificial neural network for wear investigation of ball bearing materials under pure sliding condition. *Applied Engineering Letters*, 7(2), 81-88. <https://doi.org/10.18485/aeletters.2022.7.2.5>
- [16] Grujičić, R., Tica, M., Stojanović, B., Ivanović, L., & Mitrović, R. (2022). Analysis of impact of shaft speed and external load on the radial ball bearing lubrication regimes. *FME Transactions*, 50(1), 109-120. <https://doi.org/10.5937/fme2201109G>
- [17] Petrova, A., Yaneva, S., Miteva, A., Stefanov, G., & Barbov, B. (2022). Study of oxidation kinetics of al-si alloys with high concentration of impurities (Fe, Zr, V). *Advanced Engineering Letters*, 1(1), 1-7. <https://doi.org/10.46793/adeletters.2022.1.1.1>
- [18] Kusyi, Y., Kuk, A., Onysko, O., Lukan, T., Pituley, L., Shuliar, I., & Havryliv, Y. (2020). Application of the criterion of technological damageability in mechanical engineering. *STED Journal*, 2(2), 13-21. <https://doi.org/10.7251/STED0220013K>
- [19] Tchomeni, B. X. & Alugongo, A. (2021). Modelling and Dynamic Analysis of an Unbalanced and Cracked Cardan Shaft for Vehicle Propeller Shaft Systems. *Applied Sciences*, 11(17), 8132. <https://doi.org/10.3390/app11178132>
- [20] Stanojević, M., Tomović, R., Ivanović, L., & Stojanović, B. (2022). Critical analysis of design of ravigneaux planetary gear trains. *Applied Engineering Letters*, 7(1), 32-44. <https://doi.org/10.18485/aeletters.2022.7.1.5>
- [21] Veličković, S., Djordjević, Z., Stojanović, B., Blagojević, J., & Miladinović, S. (2018). Influence of angles of fiber orientation on improving the characteristics of composite cardan shaft using factorial experiment. *IOP Conf. Series: Materials Science and Engineering*, 393, 012086. <https://doi.org/10.1088/1757-899X/393/1/012086>
- [22] Munteanu, C., Paleu, V., Istrate, B., Dascălu, A., Cîrlan Paleu, C., Bhaumik, S., & Ancaș, A. D. (2021). Tribological Behavior and Microstructural Analysis of Atmospheric Plasma Spray Deposited Thin Coatings on Cardan Cross Spindles. *Materials (Basel)*, 14(23), 7322. <https://doi.org/10.3390/ma14237322>
- [23] Rakhmatov, M. I., Zayniddinovich, S. Z., & Tuygunovich, B. M. (2022). Analysis of Cardan Shaft Defects and Ways to Restore Them. *Vital Annex: International Journal of Novel Research in Advanced Sciences*, 1(3), 135-137.
- [24] Riskulov, A. A., Rakhmatov, M. I., & Avliyokulov, J. S. (2022). To Determine the Bending Stiffness of Stand Cardan Shafts, Splined Joints of Construction and Road Vehicles. *Nexus: Journal of Advances Studies of Engineering Science*, 1(3), 40-44.
- [25] Šalinić, S., Vranić, A., Nešić, N. D., & Tomović, A. M. (2017). On the Torque Transmission by a Cardan-Hooke Joint. *FME Transactions*, 45(1), 117-121. <https://doi.org/10.5937/fmet1701117>
- [26] Rakić, M. B., Ivanović, L., Josifović, D., Stojanović, B., & Ilić, A. (2013). The influence of variation in position of output shaft to load on the cardan joint cross shaft. *Mobility & Vehicle Mechanics*, 39(1), 53-64.
- [27] VDI 2722 (2003). *Cardan shafts and Cardan shaft lines - Homokinematic mechanisms.* Verein Deutscher Ingenieure.
- [28] Chaban, A., Lukasik, Z., Popena, A., & Szafraniec, A. (2021). Mathematical Modelling of Transient Processes in an Asynchronous Drive with a Long Shaft Including Cardan Joints. *Energies*, 14(18), 5692. <https://doi.org/10.3390/en14185692>
- [29] Ašonja, A., Desnica, E., Pastukhov, A., Kuznetsov, Y., & Kravchenko, I. (2023). Method for Quick Determination of the Reliability Level of Agricultural PTO Shafts. *Lecture Notes in Networks and Systems*, 592, 143-149. https://doi.org/10.1007/978-3-031-21429-5_13
- [30] Sigaev, A. M., Pastukhov, A. G., & Chehunov, O. A. (2003). Cardan Joint. MIIK 7 F 16 D 3/26, 3/41, F 16 C 11/06, published 27.05.2003, №.15. Patent RU2205304.
- [31] Kuznetsov, Y. A., Selemenev, M. F., Kravchenko, I. N., Spasibin, A. V., & Pankov, G. B. (2022). Theoretical Justification of Coating Adhesion during Gas-Thermal Spraying. *Materials Research Proceedings*, 21, 161-168. <https://doi.org/10.21741/9781644901755-29>
- [32] Erokhin, M. N. & Pastukhov, A. G. (2008). *Reliability of Cardan Shaft in Transmissions of Agricultural Engineering in Exploitation.* Belgorod State Agricultural Academy, Belgorod, Russia.
- [33] Pastukhov, A., Timashov, E., Kravchenko, I., & Parnikova, T. (2020). Adaptivity of thermal diagnostics method of mechanical transmission assemblies. *Proceedings of Scientific Conference "Engineering for Rural Development"*, 18, 107-113. <https://doi.org/10.22616/ERDev.2020.19.TF024>

Contact information:

Eleonora DESNICA, Full Professor
(Corresponding author)
University of Novi Sad, Technical Faculty "Mihajlo Pupin",
Đure Đakovića bb, 23000 Zrenjanin, Republic of Serbia
E-mail: desnica@tfzr.uns.ac.rs

Aleksandar AŠONJA, Associate Professor
University Business Academy in Novi Sad,
Faculty of Economics and Engineering Management in Novi Sad,
Cvecarska 2, 21000 Novi Sad, Republic of Serbia
E-mail: asonja.aleksandar@fimek.edu.rs

Milan KLJAJIN, Full Professor with Tenure
University North, University Center Varaždin,
Jurja Križanića 31b, 42000 Varaždin, Croatia
E-mail: mkljajin@unin.hr

Hrvoje GLAVAŠ, Associate Professor
University of Osijek, Faculty of Electrical Engineering,
Computer Science and Information Technology Osijek,
Kneza Trpimira 2B, 31000 Osijek, Croatia
E-mail: hrvoje.glavas@ferit.hr

Alexander PASTUKHOV, Full Professor
Belgorod State Agricultural University named after V. Gorin,
Vavilova 1, Mayskiy 308503, Belgorod region, Russian Federation
E-mail: pastukhov_ag@mail.ru